9(2012) 657 – 673

Latin American Journal of Solids and Structures

www.lajss.org

Active vibration control of a piezoelectric beam using PID controller: Experimental study

Abstract

Vibration suppression of smart beams using the piezoelectric patch structure is presented in the present work. The smart system consists of a beam as the host structure and piezoceramic patches as the actuation and sensing elements. An experimental set-up has been developed to obtain the active vibration suppression of smart beam. The set-up consists of a smart cantilever beam, the data acquisition system and a LabView based controller. Experiments are performed for different beam specimen. The coupled efficient layerwise (zigzag) theory is used for theoretical finite element modeling. The finite element model is free of shear locking. The beam element has two nodes with four mechanical and a variable number of electric degrees of freedom at each node. In the thickness direction, the electric field is approximated as piecewise linear across an arbitrary number of sub-layers in the piezoelectric layers. Cubic Hermite interpolation is used for the deflection, and linear interpolation is used for the axial displacement and the shear rotation. Undamped Natural Frequencies are obtained by solving the Eigen Value problem using Subspace Iteration method for cantilever beam. A state space model characterizing the dynamics of the physical system is developed from experimental results using PID approach for the purpose of control law design. The experimental results obtained by using the active vibration control system have demonstrated the validity and efficiency of PID controller. Experiments are conducted to compare the controlling of various cantilever beams of different sizes. It shows that the present actuator and sensor based control method is effective and the LabView control plots for various beams can be used as a benchmark for analytical work. The results are compared with ABAQUS software and 1D Finite element formulation based on zigzag theory.

Keywords

Zig-zag theory, LabView, 2D ABAQUS, PID controller, FEM.

Najeeb ur Rahman* **and M. Naushad Alam**

Department of Mechanical Engineering, Aligarh Muslim University, Aligarh,U.P-202002, India.

Received 30 Apr 2012;
In revised form 24 May 2012

* Author email: najeebalig@rediffmail.com

1 INTRODUCTION

The concept of smart or intelligent structures has started a new structural revolution. A smart structure typically consists of a host structure incorporated with sensors and actuators coordinated by a controller. The integrated structure system is called a smart structure because it has the ability to perform self-diagnosis and adapt to the environment change. For active vibration control, the design of piezoelectric smart structures need both the structural dynamics and control theories to be considered. The finite element method proved to be a powerful tool for analyzing such complex structures. The effectiveness of active control depends on the mathematical model and control strategy. Baz and Poh [3] presented a modified independent modal space control (MIMSC) method. By using this method one piezoelectric actuator can control several modes at the same time.

Sun et al. [17] proposed a hybrid control algorithm to control the rotation of a flexible beam while suppressing the beam's vibration. The control law combines an enhanced PD feedback with a nonlinear differentiator to derive a high-quality velocity signal to control the gross motion of the beam and a vibration control by PZT actuators bonded on the surface of the beam. Experimental and numerical results validate these theoretical analyses and control methods. However the aim of vibration control for distributed parameter system is to design the control methods based only on a limited number of modes that use much small numbers of actuators/sensors to control a large dimensional system. When the excitation of the residual modes by the actuators is the result of the active control system this is known as control spillover [13].Control spillover may occur if high frequency dynamics is ignored by modal truncation and spillover will cause instability in the closed-loop system [6]. Choi et al.[5] formulated a new discrete time sliding mode controller and conducted experimental researches to alleviate chattering in vibration control of smart structures and also to achieve robustness to the system. To measure and control vibrations, an accelerometer is often used as sensor in flexible structures. Acceleration is often easier to measure than displacement or velocity. Gatti et al.[7] conducted active damping of a beam using physically collocated accelerometer and piezoelectric patch actuator. Preumont[16] addressed the case in which the output of the system is the acceleration and the control input is a force by using collocated actuator and sensor pairs. He presented a compensator involving a second-order filter which also enjoys guaranteed stability and exhibits a larger roll-off at high frequency. He then considered the case of a single degree of freedom oscillator and extended the results to SISO systems with many modes and to MIMO systems. When considering a flexible axis under PID control a root locus study shows that the closed-loop bandwidth is limited by the open-loop anti-resonance and that there exists a maximum closed-loop damping ratio that depends on the inertia ratio whatever the values of the control parameters [8].Therefore classical tuning of PID controllers using pole-placement or optimization criteria based on a periodic and minimum-phase models are not applicable to flexible mechanical structures. However in a number of specific cases the adequate PID parameters can be found with optimization techniques for determining speed loop PID parameters by minimizing an ITAE criterion or assuming the existence of multiple roots [18]. In the case of flexible axes PID control these analytical methods are difficult to

work out when high uncertainties on model parameters exist. Zhi-cheng et al. [4] presented the theoretical analysis and experimental results of active vibration suppression of a flexible beam with bonded discrete PZT patches sensors / actuators and mounted accelerometer.

To predict the response of laminates more accurately, many models have been developed on the basis of kinematic assumptions. In a new class of laminate theory, called the First Order Zigzag Theory (FZZT), in plane displacements in a laminate are assumed to be piecewise (Layer-wise) linear and continuous through the thickness, yet the total number of degrees of freedom is only five (doesn't depend on the number of layers). This is accomplished by analytically satisfying the transverse shear stress continuity conditions at each interface in the laminate. This theory claims to be very accurate for many cases, especially symmetric laminates. Significant improvements have been made to the FZZT [1]. The primary improvement was achieved by superimposing a piecewise linear variation of in-plane displacements on a continuous cubic function of the transverse coordinate , creating a displacement field that can better account for the warping that occurs during bending of asymmetric laminates. Kapuria and Alam [9] have developed a novel coupled zigzag theory for linear static and dynamic analysis of hybrid beams under electro-mechanical load which was extended to the linear static analysis of hybrid plate. Yang and Zhifei [19] presented state-space differential quadratic method (SSDQM) is extended to study the free vibration of a functionally graded piezoelectric material (FGPM) beam under different boundary conditions. The FGPM beam is approximated as a multi-layered cantilever. Kapuria and Yasin [10] used layerwise plate theory and proposed the active vibration suppression of hybrid composite and fiber metal laminate (FML) plates integrated with piezoelectric fiber reinforced composite (PFRC) sensors and actuators. Zabihollah et al. [20] developed a finite element model based on the layerwise displacement theory which incorporates the electro-mechanical coupling effects. They developed an experimental set-up to determine the natural frequency and damping factor of the smart laminated beam and compared the results with simulation results.

The present work intends to investigate the vibration suppression of smart cantilever beams which consists of a beam as the host structure and piezoceramic patches as the actuation and sensing elements. An experimental set-up has been developed to obtain the active vibration suppression of smart beam. The experimental results are compared with 1D-FE and 2D-FE results.

2 STRUCTURAL MODELING

2.1 The coupled zig-zag beam theory approximations

Consider a hybrid beam as shown in Fig. 1. The thickness of the beam varies segment wise due to the presence of piezoelectric patches. The bottom and top surfaces of the beam are $z = z_0$ and $z = z_L$ planes, which may vary segment-wise. All the elastic and piezoelectric layers are perfectly bonded. It is loaded transversely on the bottom and top with no variation along the width b. The piezoelectric layers have poling direction along z-axis. The approximations of the coupled zigzag theory [9] are as follows.

A state of plane stress is assumed i.e. $\sigma_y = \tau_{xy} = \tau_{yz} = 0$ for a beam with a small width. A plane strain state $\varepsilon_y = \gamma_{yz} = \gamma_{xy} = 0$ is considered for infinite panels. The transverse normal stress, σ_z is neglected. The axial displacement, u, transverse displacement, w and electric potential ϕ are assumed to be independent of y. With these assumptions, the general 3D constitutive equations of a piezoelectric medium for stresses σ_x, τ_{zx} and electric displacements D_x , D_y reduce to

$$\begin{aligned} \sigma_x &= \hat{Q}_{11}\varepsilon_x - \hat{e}_{31}E_z \qquad \tau_{zx} = \hat{Q}_{55}\gamma_{zx} - \hat{e}_{15}E_x \\ D_x &= \hat{e}_{15}\gamma_{zx} + \hat{\eta}_{11}E_x \qquad D_z = \hat{e}_{31}\varepsilon_x + \hat{\eta}_{33}E_z \end{aligned} \tag{1}$$

where $\hat{Q}_{11}$,$\hat{Q}_{55}$; $\hat{e}_{31}$,$\hat{e}_{15}$;$\hat{\eta}_{11}$,$\hat{\eta}_{33}$ are the reduced stiffness coefficients, piezoelectric stress constants and electric permittivities.

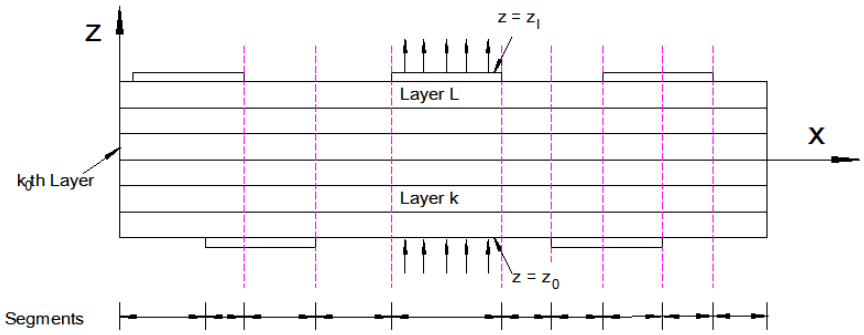

Figure 1 Geometry of hybrid beam

The potential field ϕt time t is assumed as piecewise linear between $n_\phi$oints z_φ^j across the thickness [12]:

$$\phi(x,z,t) = \Psi_\phi^j(z)\,\phi^j(x,t) \tag{2}$$

where $\phi^j(x,t) = \phi\left(x, z_\phi^j, t\right)\Psi_\phi^j(z)$ are linear interpolation functions. The variation of deflection ws obtained by integrating the constitutive equation for ε_z by neglecting the contribution of σ_x via Poisson's effect compared to that due to the electric field: $w_{,z} \simeq -d_{33}\phi_{,z} \Rightarrow$

$$w(x,z,t) = w_0(x,t) - \bar{\Psi}_\phi^j(z)\,\phi^j(x,t) \tag{3}$$

where $\bar{\Psi}_\phi^j(z) = \int_0^z d_{33}\Psi_{\phi,z}^j(z)\,dz$ is a piecewise linear function. The axial displacement u for the k^{th} layer is approximated to follow a global third order variation across the thickness with a layerwise linear variation

$$u(x,z,t) = u_0(x,t) - zw_{0,x}(x,t) + z\psi_k(x,t) + z^2\xi(x,t) + z^3\eta(x,t) \tag{4}$$

u_0 and ψ_0 are the axial displacement and the shear rotation at $z = 0$, respectively. Using the $(L-1)$ conditions each for the continuity of τ_{zx} and u at the layer interfaces and the two

shear traction-free conditions $\tau_{zx} = 0$ at $z = \pm h/2$, the functions u_k, ψ_k, ξ, η are expressed in terms of u_0 and ψ_0 to yield

$$u(x,z,t) = u_0(x,t) - zw_{0,x}(x,t) + R^k(z)\psi_0(x,t) + R^{kj}(z)\phi^j_{,x}(x,t) \tag{5}$$

where $R^{kj}(z)$, are cubic functions of z whose coefficients are dependent on the material properties and lay-up. Eqs. (5) and (3) for u, w can be expressed as

$$u = f_1(z)\bar{u}_1 w = f_2(z)\bar{u}_2 \tag{6}$$

With

$$\bar{u}_1 = \begin{bmatrix} u_0 & -w_{0,x} & \psi_0 & \phi^j_{,x} \end{bmatrix}^{\mathrm{T}}, \bar{u}_2 = \begin{bmatrix} w_0 & -\phi^j \end{bmatrix}^{\mathrm{T}} \tag{7}$$

$$f_1(z) = \begin{bmatrix} 1 & z & R^k(z) & R^{kj}(z) \end{bmatrix}, f_2(z) = \begin{bmatrix} 1 & \bar{\Psi}^j_\phi(z) \end{bmatrix} \tag{8}$$

where elements with index j mean a sequence of elements with j = 1 to n_ϕ. Using Eqs. (6) and (2), the strains and the electric fields can be expressed as

$$\begin{array}{ll} \varepsilon_x = u_{,x} = f_1(z)\bar{\varepsilon}_1, & \gamma_{zx} = u_{,z} + w_{,x} = f_5(z)\bar{\varepsilon}_5. \\ E_x = -\phi_{,x} = -\Psi^j_\phi(z)\phi^j_{,x}(x), & E_z = -\phi_{,z} = -\Psi^j_\phi(z)\phi^j(x) \end{array} \tag{9}$$

2.2 Hamilton's Principle

Let p^1_z, p^2_z be the normal forces per unit area on the bottom and top surfaces of the beam in direction z. Let there be distributed viscous resistance force with the distributed viscous damping coefficient c_1 per unit area per unit transverse velocity of the top surface of the beam. At the interface at $z = z^{ji}_\phi$ where the potential is prescribed, the extraneous surface charge density is q_{ji}. Using the notation $\ldots = \sum_{k=1}^{L} \int_{z^+_{k-1}}^{z^-_k} (\ldots)\, b\mathrm{d}z$ for integration across the thickness, the extended Hamilton's principle for the beam reduces to

$$\int_x \left[\begin{array}{c} \rho u\,\delta u + \rho w\,\delta w + \sigma_x\delta\varepsilon_x\tau_{zx}\delta\gamma_{zx} - D_x\delta E_x D_z\delta E_z - bp^1_z\delta w(x,z_0,t) \\ -b\left\{p^2_z - c_1\dot{w}(x,z_L,t)\right\}\delta w(x,z_L,t) + bD_z(x,z_0,t)\,\delta\phi^1 - bD_z(x,z_L,t)\,\delta\phi^{n_\phi} \\ -bq_{ji}\delta\phi^{ji} \end{array} \right] \mathrm{dx} \\ -\langle \sigma_x\delta u + \tau_{zx}\delta w + D_x\delta\phi \rangle\, x = 0 \tag{10}$$

Substituting the expressions (6) and (2) for u, w, ϕ and (9) for ε_x, γ_{zx}, E_x, E_z into Eqn (10) yields

$$\int_x \left[\begin{array}{c} \delta\bar{u}^T_1 I\,\bar{\bar{u}}_1 + \delta\bar{u}^T_2\bar{I}\,\bar{u}_2 + \delta\bar{\varepsilon}^T_1 F_1 + \delta\bar{\varepsilon}^T_5 F_5 + \delta\phi^j_{,x}H^j + \delta\phi^j G^j - \left(F_2 - \hat{F}_2\right)\delta w_0 \\ -\left(F^j_4 - \hat{F}^j_4\right)\delta\phi^j \end{array} \right] \mathrm{dx} \\ -[\bar{N}_x\delta\bar{u}_0 + \bar{V}_x\delta\bar{w}_0 - \bar{M}_x\delta\bar{w}_{0,x} + \bar{P}_x\delta\bar{\psi}_0 + \left(\bar{H}^j - \bar{V}^j_\phi\right)\delta\bar{\phi}^j + \bar{S}^j_x\delta\phi^j_{,x}]|_x = 0 \tag{11}$$

where an over-bar on the stress and electric resultants and on u_0, w_0, ψ_0, ϕ^j means values at the ends. In this equation, I, $\bar{I}$ are the inertia matrices, F_1 is the stress resultant of σ_x; F_5, V_x, V_ϕ^j are the stress resultants of τ_{zx} and H^j, G^jf D_x, D_z are the electric resultants [12].

2.3 Finite element model

A two noded beam element based on the efficient layerwise zigzag theory is presented in this section. Each node has four mechanical and a variable number of electric degrees of freedom. Cubic Hermite interpolation is used for expending w_0, ϕ^j in terms of the nodal values of w_0, $w_{0,x}$ and ϕ^j, $\phi^j_{,x}$ respectively, and a linear interpolation is used for u_0, ψ_0

The element generalized displacement vector U^e defined as

$$U^{eT} = \begin{bmatrix} u_0^{eT} & w_0^{eT} & \psi_0^{eT} & \phi^{eT} \end{bmatrix} \tag{12}$$

The contribution T^ef an element to the integral in Eq. (11) is obtained as

$$T^e = \int_0^a \left[\delta\hat{u}^T \hat{I}\, \ddot{\hat{u}} + \delta\hat{\varepsilon}^T \hat{D}\hat{\varepsilon} - \delta\hat{u}^T f_{u\phi} + \delta\hat{u}^T \hat{C}\, \dot{\hat{u}} \right] dx \tag{13}$$

Substituting the expressions for $\hat{u}$ and $\hat{\varepsilon}$ T^e can be expressed as

$$T^e = \int_0^a \delta U^{e^T} \left[\hat{N}^T \hat{I} \hat{N} \ddot{U}^e + \hat{N}^T \hat{C} \hat{N} \dot{U}^e + \hat{B}^T \hat{D} \hat{B} U^e - \hat{N}^T f_{u\phi} \right] dx. \tag{14}$$

with

$$K^e = \int_0^a \hat{B}^T \hat{D} \hat{B} dx, \;\; P^e = \int_0^a \hat{N}^T f_{u\phi} dx.. \tag{15}$$

Summing up contributions of all elements to the integral in Eq. (11), the system equation can be obtained as

$$M\ddot{U} + C\dot{U} + KU = P \tag{16}$$

in which M, C, K are assembled from the element matrices $M^e C^e$, K^end U, P are the assembled counterparts of U^e, P^e. the mechanical boundary conditions for beam are

$$Clampedend: u_0 = 0, \;\; w_0 = 0, \;\; w_{0,x} = 0, \;\; \psi_0 = 0, \tag{17}$$

$$\text{Free end: } N_x = 0, \;\; V_x = 0, \;\; M_x = 0, \;\; P_x = 0.$$

2.4 Dynamic Response and Modal Analysis:

The electromechanical inertia and damping terms in M d Can be neglected for the purpose of computational efficiency [12]. Considering this, Eq. (16) can be partitioned and arranged for open circuit condition as

$$\begin{bmatrix} M^{uu} & 0 & 0 \\ 0 & 0 & 0 \\ 0 & 0 & 0 \end{bmatrix} \begin{Bmatrix} \ddot{\bar{U}} \\ \ddot{\Phi}_s \\ \ddot{\Phi}_a \end{Bmatrix} + \begin{bmatrix} C^{uu} & 0 & 0 \\ 0 & 0 & 0 \\ 0 & 0 & 0 \end{bmatrix} \begin{Bmatrix} \dot{\bar{U}} \\ \dot{\Phi}_s \\ \dot{\Phi}_a \end{Bmatrix} + \begin{bmatrix} K^{uu} & K^{us} & K^{ua} \\ K^{su} & K^{ss} & 0 \\ K^{au} & 0 & K^{aa} \end{bmatrix} \begin{Bmatrix} \bar{U} \\ \Phi_s \\ \Phi_a \end{Bmatrix} = \begin{Bmatrix} \bar{P} \\ 0 \\ Q_a \end{Bmatrix} \tag{18}$$

Where, the system vector U is partitioned into vectors of mechanical displacements $\bar{u}$, unknown output voltages ϕ_s and known input actuation voltages ϕ_a Correspondingly, P is partitioned into vectors of mechanical loads $\overline{P}$ known electric loads Q_s and unknown output electrical loads Q_a

Eq. (18) is the generalised equation of dynamics obtained through finite element model using Hamilton principle based on zig zag theory. It is used for controlling various parameters by considering different conditions. Here in this study, the output voltage. ϕ_s, for open circuit condition, is obtained as follows:

$$\Phi_s = -\left(K^{ss}\right)^{-1} K^{su} \bar{U}. \tag{19}$$

Substitution of Eq. (19) into Eq. (18) yields

$$M^{uu}\ddot{\bar{U}} + C^{uu}\dot{\bar{U}} + \left[K^{uu} - K^{us}\left(K^{ss}\right)^{-1} K^{su}\right]\bar{U} = \bar{P} - K^{ua}\Phi_a. \tag{20}$$

For un-damped free vibration, the damping matrix C^{uu} and the right-hand side vector of the above equation are set to zero. The resulting generalised Eigen-value problem is solved using subspace iteration method [16] to obtain the un-damped natural frequencies ω for transient response, Eq. (20) is solved using Newmark direct time integration method [15]. The equation of motion for un-damped free vibration can be extracted from finite element model, for modal analysis as

$$M^{uu}\ddot{\bar{U}} + \left[K^{uu} - K^{us}\left(K^{ss}\right)^{-1} K^{su}\right]\bar{U} = 0 \tag{21}$$

$$M^{uu}\bar{U} + K_{mod}\bar{U} = 0 \tag{22}$$

where $K_{mod} = \left[K^{uu} - K^{us}\left(K^{ss}\right)^{-1} K^{su}\right]$ is the modified stiffness of the host structure due to piezoelectric effect. The solution of this equation is assumed of the form

$\bar{U} = U_0 e^{j\omega t}$where $j = \sqrt{-1}$

Substituting it in equation (22)

$$\left[K_{mod} - \omega^2 M^{uu}\right] = 0 \tag{23}$$

The non trivial solution of this equation exist if

$$\left|K_{mod} - \omega^2 M^{uu}\right| = 0 \tag{24}$$

The equation (24) is called the characteristic equation and its roots are called the Eigen values which give the natural frequencies of the system. Thus there are n values of natural frequencies of the system $\omega = diag\left(\omega_1\ \omega_2\ \omega_3 \ldots \omega_n\right)$ and ω_i is the i^{th} natural frequency of the system.

3 PID CONTROLLER

The block diagram of a simplified PID controller in a closed loop system is shown in Fig. 2 [2, 12]. In practice the output of a PID controller is given by Eq. (25) [11, 14].

$$u(t) = Kp\left\{e(t) + \frac{1}{T_i}\int_0^t e(t)dt + Td\frac{de(t)}{dt}\right\} \tag{25}$$

The transfer function of of a PID controller is

$$Gpid(s) = \frac{U(s)}{E(s)} = K_p + \frac{k_i}{s} + Kds = K_p(1 + \frac{1}{T_{is}} + Tds) \tag{26}$$

Where K_p= Proportional gain, T_i= integral time, and T_d= derivative time. The main task of the controller tuning is to succeed high and desirable performance characteristics using the approach of determining the PID controller parameters. In the design of PID controller for active vibration control of beam, three parameters are specified in LabView block diagram: proportional gain (Kp), integral gain (Ki), and derivative gain (Kd). The performance of the controller directly depends on these parameters. In order to obtain the desired system response, these parameters must be optimally adjusted. For this aim the optimal values of K_p, K_i and K_d are respectively adjusted as 2.45, 1 and 1.

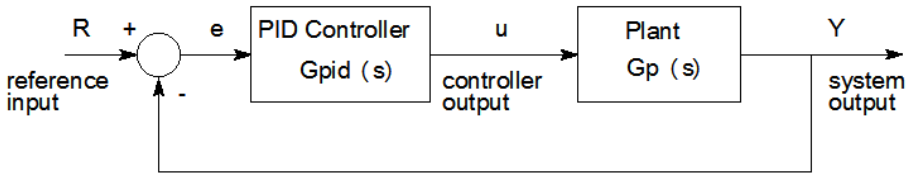

Figure 2 Block diagram of PID controller

The variable (e) represents the tracking error, the difference between the desired input value (R) and the actual output (Y). This error signal (e) will be sent to the PID controller, and the controller computes both the derivative and the integral of this error signal. This signal (u) 12 will be sent to the plant, and the new output (Y) will be obtained. This new output (Y) will be sent back to the sensor again to find the new error signal (e). The controller takes this new error signal and computes its derivative and it's integral again. This process goes on and on for the closed system.

4 RESULTS AND DISCUSSIONS

4.1 Experimental and Numerical works

For the experimental and numerical evaluation, the following three cantilever beam specimens are considered:

(a) An Al Beam of size 300mm × 25mm × 2.2mm, with a PZT-5H piezo-ceramic sensor (20mm × 20mm × 0.4mm) bonded to the top surface near to the fixed end and a PZT-5H piezo-

ceramic actuator of the same size bonded symmetrically to the bottom surface of the host beam (Fig. 3).

(b) An Al Beam of size 180mm × 27mm × 2mm, with a PZT-5H piezo-ceramic sensor (15mm × 15mm × 0.5mm) bonded to the top surface near to the fixed end and a PZT-5H piezo-ceramic actuator (15mm × 15mm × 0.5mm) bonded symmetrically to the bottom surface of the host beam (Fig. 4).

(c) A Composite Beam comprising of top and bottom Al layers of size 500mm×30mm×1mm and intermediate glass fibre core of size 500mm×30mm×2mm, with a PZT-5H piezo-ceramic sensor (50.8mm×25.4mm×0.5mm) bonded to the top surface near to the fixed end and a PZT-5H piezo-ceramic actuator of the same size bonded symmetrically to the bottom surface of the host beam (Fig. 5).

Figure 3 Specimen Beam (a) of size 300mm×25mm×2.2mm

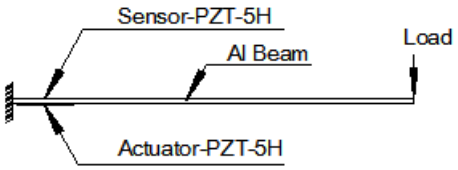

Figure 4 Specimen Beam (b) of size 180mm×27mm×2mm

Figure 5 Specimen Beam (c) of size 500mm×30mm×4mm

The properties of materials used in the configuration of beams are described in Table 1.

The experimental set-up consists of a smart cantilever beam (Fig. 3,4 and 5), a piezo-sensing system, a piezo-actuation system, a data acquisition board (SCB-68, National Instruments), connecting wires/cables and a PC computer loaded with LabView 8.6 (National Instruments). The physical and schematic experimental setups are shown in Fig. 6 and Fig. 7 respectively. In the set-up for measuring the sensor voltage, a piezo-sensing system is used. The signal conditioning module conditions the electrical signals acquired by sensor so as they are in a form that the DAQ device can accept. DAQ device acquire a real-world signal such as

Table 1 Material properties

Elastic Properties										
Material	E_1	E_2	E_3	G_{12}	G_{23}	G_{13}	ν_{12}	ν_{13}	ν_{23}	ρ
	GPa									Kg/m^{-3}
Glass Fibre	11.04	11.04	6.75	1.57	1.53	1.53	0.12	0.32	0.32	2500
Aluminium	68	68	68	25.758	25.758	25.758	0.32	0.32	0.32	2800
PZT-5H	60.60	60.60	48.309	22.988	22.988	22.988	0.3182	0.0636	0.3182	7500

Piezoelectric Strain constants and Electric Permittivity								
Material	d_{31}	d_{32}	d_{33}	d_{15}	d_{24}	e_{11}	e_{22}	e_{33}
	$(\times 10^{-12} mV^{-1})$					$(\times 10^{-12} Fm^{-1})$		
PZT-5H	-274	-274	593	741	741	3130	3130	3400

a voltage signal and inputs the signal into the computer for processing, analysis, storage, and other data manipulations. Physical phenomena represents the real world signal that we are trying to measure, such as speed, temperature, vibration, and light intensity etc. Sensors are used to evaluate the physical phenomena and produce proportionate electrical signals. Piezoelectric patch, used in the present setup, is a type of sensor that converts the beam vibration into the voltage signal that an analog to digital (A/D) converter can measure. The electrical signal produced by the sensors is fed to the controller through DAQ.

The controller inbuilt in the LabView processes the signal and gives command to DAQ device (SCB-68) to read digital input signal which converts it into an analog output signal (D/A conversion) and that output signal is fed to the piezo-actuation system. The amplified analog signal from piezo-actuation system goes to the piezo-ceramic patch known as actuator to control the beam vibration.

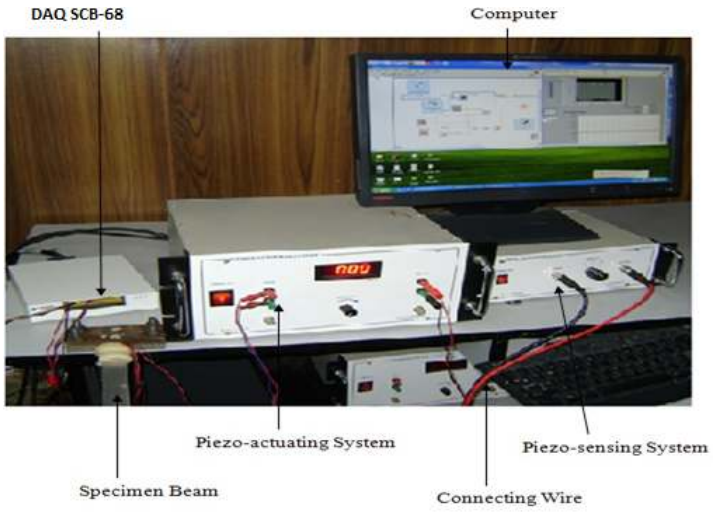

Figure 6 Overview of Experimental set-up

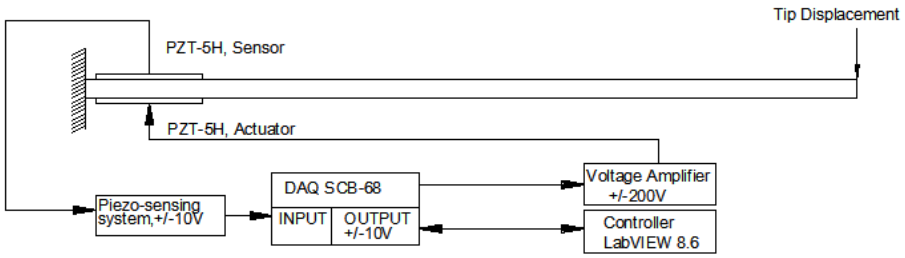

Figure 7 Schematic diagram of the experimental set-up

4.1.1 Experimental open-loop response

To obtain the free vibration response of the smart beam the initial tip displacement of magnitude 2.5 cm is applied. When the free vibrations in the beam start, the sensor deforms and due to the piezoelectric property of piezo-ceramic material, the sensor produces an electrical signal of low magnitude which is fed to the piezo-sensing system. The piezo-sensing system amplify the PZT-5H sensor signal to the voltage range of -10 to +10V with frequency range of 1-10 kHz. The piezo-sensing system output is fed to the data acquisition board consisting of A/D interface and the amplitude (voltage) vs. Time (Sec) response is obtained using LabView 8.6 (Fig.8, 9 and 10).

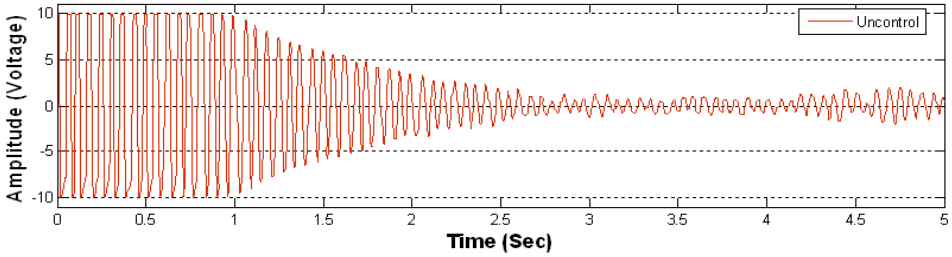

Figure 8 Experimental Un-control Vibration of beam (a)

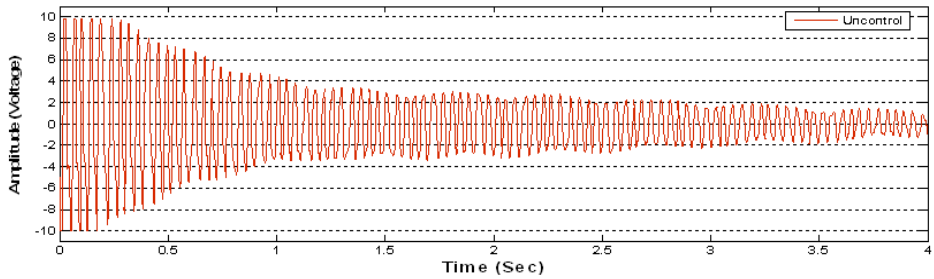

Figure 9 Experimental Un-control Vibration of beam (b)

Using the experimental response of the beam (a), it is noted that 79 cycles are realized in the time interval 4.9525 sec. Thus the natural frequency of beam (a) is $\omega = (79/4.9525) = 15.9515$Hz. Using the same time interval the damping co-efficient is determined by computing

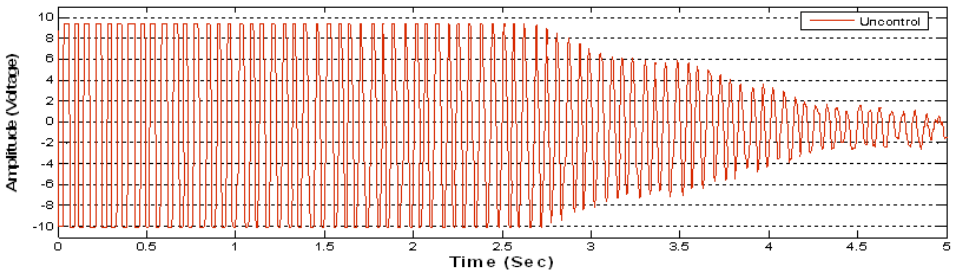

Figure 10 Experimental Un-control Vibration of beam (c)

the logarithmic decrement δ as 0.0274 and the damping factor $\xi = 0.0658$. Similarly the natural frequency, logarithmic decrement and damping factor of the other two beams are determined and listed in Table 2.

Table 2 Experimental open-loop natural frequency, logarithmic decrement and damping factor of cantilever beams

Specimen Beam	Specifications Beam	Natural Frequency (Hz)	Logarithmic decrement δ	Damping Factor (ξ)
Beam (a)	Aluminium $(300\times3\times25)\,\mathrm{mm}^3$	15.962	0.0274	0.00436
Beam (b)	Aluminium $(180\times3\times27)\,\mathrm{mm}^3$	24.615	0.0242	0.00385
Beam (c)	Composite $(500\times5\times30)\,\mathrm{mm}^3$	16.20	0.0279	0.00444

The experimental value of damping co-efficient is of great importance to design the control strategy as it directly affects the state matrices. The three experimental beams are than modeled in 2D FE (ABAQUS) and 1D FE (Matlab) and natural frequencies are obtained and validated by comparing with experimental results in Table-3. For the 2D-FE analysis, beam (a) and (c) have been modeled with 1600 eight-noded isoparametric plane stress elements for span to thickness ratio, S = 100 and beam (b) has been modeled with 1200 elements for S = 60. The results obtained using twice the above number of elements is found to be indistinguishable from these results. 1D FE results are obtained using 20 equal sized two noded elements.

It is observed that the 2D-FE and 1D FE results are in excellent agreement with experimental results. Further the corresponding mode shapes of the three beams obtained using 2D plane stress finite element results, using ABAQUS, are presented in Figs. (11,12,13). The mode shapes of the Al beams (beam (a) and (b)) are almost identical due to the same beam material whereas for the composite beam (beam (c)), it is different due to more flexibility of glass fibre.

Table 3 Comparison of experimental open-loop natural frequency of cantilever beams with 2D-FE and 1D-FE results.

		Natural Frequency (Hz)		
Specimen Beam	Beam Specifications	Experimental (LabView)	2D-FE (ABAQUS)	1D-FE (MatLab)
Beam (a)	Aluminium $(300\times3\times25)\,\mathrm{mm}^3$	15.962	15.159	16.01
Beam (b)	Aluminium $(180\times3\times27)\,\mathrm{mm}^3$	24.615	26.009	26.775
Beam (c)	Composite $(500\times5\times30)\,\mathrm{mm}^3$	16.20	16.608	17.071

Figure 11 Mode shape of beam (a) using 2D-FE (ABAQUS)

Figure 12 Mode shape of beam (b) using 2D-FE (ABAQUS)

Figure 13 Mode shape of beam (c) using 2D-FE (ABAQUS)

4.1.2 Experimental closed-loop response

To demonstrate the control strategy, the set-up utilized in section 4 has been used. A push button is simulated in the LabView to activate the controller. A 2.5 cm initial displacement has been applied at the tip of the beam and the beam is suddenly released. The sensor signal passing through the piezo-sensing system and DAQ is fed to the controller. The PID controller is configured to process the input signal from DAQ and it generates an appropriate output signal through PID algorithm. The controller response goes into DAQ (consisting of D/A interface) and the DAQ output is fed to the piezo-actuation system. The piezo-actuation system amplifies a low voltage input signal in the range of -10 to +10V to a high voltage output signal in the range of -200V to +200V and the frequency range of 1-2000Hz. The amplified signal is fed directly to the PZT-5H piezo-actuator which due to the piezoelectric properties of PZT material, produces the mechanical effect to perform closed loop control of the structure by automatic modification of the system's structural response. Figs. (14-16) show the plots of experimental open loop vs. closed-loop response of the three beams.

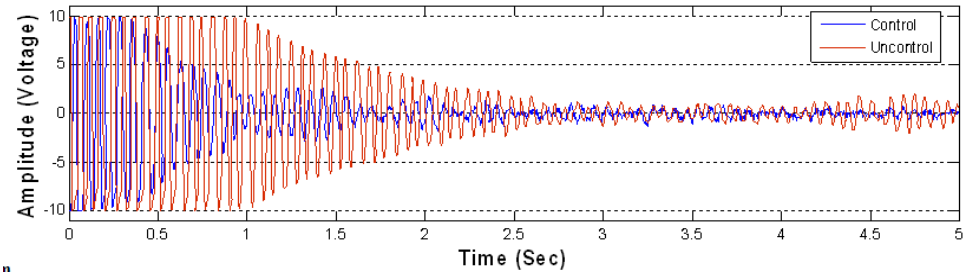

Figure 14 Experimental open-loop vs. closed-loop vibration response of Beam (a)

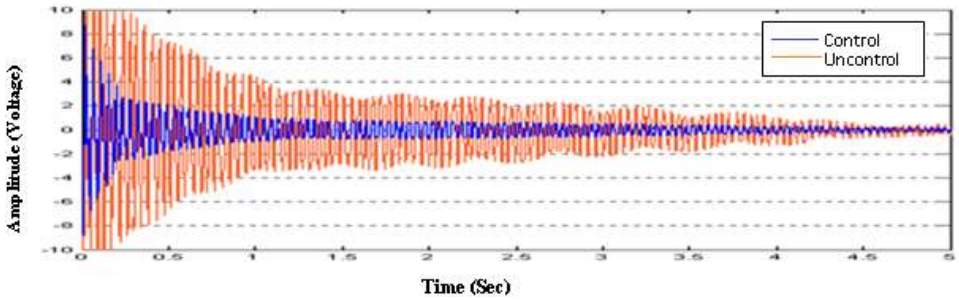

Figure 15 Experimental open-loop vs. closed-loop Vibration response of Beam (b)

Using the experimental closed-loop response of the beam (a), it is noted that 48 cycles are realized in the time interval 3.1 sec. Thus the natural frequency of beam (a) is $\omega = (48/3.1) = 15.484$Hz, which is in excellent match with the natural frequency result obtained using open-loop response. Using the same time interval, the logarithmic decrement δ is determined as 0.0547 and the damping factor $\xi = 0.0087$. Similarly the natural frequency, logarithmic decrement and damping factor of the other two beams are determined and listed in Table-

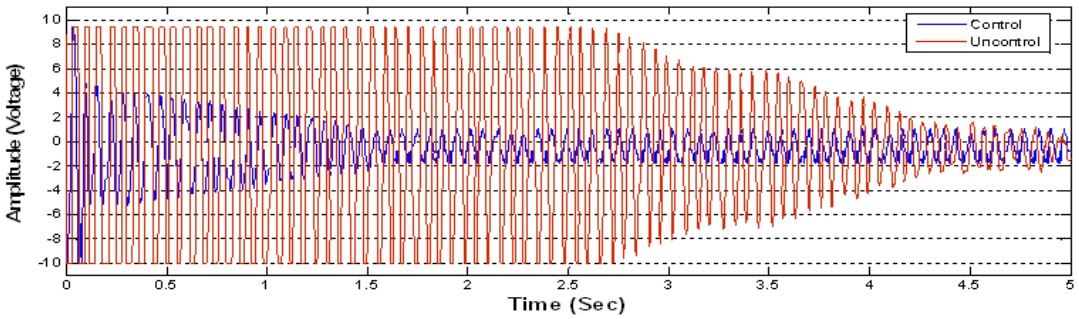

Figure 16 Experimental open-loop vs. closed-loop vibration response of Beam (c)

4. On comparison of results listed in Table-2 and Table-4, it may be observed that the PID controller has maintained the natural frequency of the beams and increased the damping factor to almost double its value as in open loop response. This shows the effectiveness of LabVIEW as a controller with piezoelectric beam.

Table 4 Experimental closed-loop natural frequency, logarithmic decrement and damping factor of cantilever beams

Specimen Beam	Specifications Beam	Natural Frequency (Hz)	Logarithmic decrement δ	Damping Factor (ξ)
Beam (a)	Aluminium $(300{\times}3\times25)\,\mathrm{mm}^3$	15.484	0.0547	0.0087
Beam (b)	Aluminium $(180{\times}3\times27)\,\mathrm{mm}^3$	24.051	0.0377	0.0060
Beam (c)	Composite $(500{\times}5\times30)\,\mathrm{mm}^3$	16.207	0.0509	0.0081

Figs. (17, 18, 19) show the amplitude-frequency response of the three beams with an extended frequency range. It is observed that the mode value of amplitude with control is lesser than the corresponding value without control at almost all frequencies. This difference in amplitude increases with increase in frequency. This shows the effectiveness of PID controller for a wider frequency range.

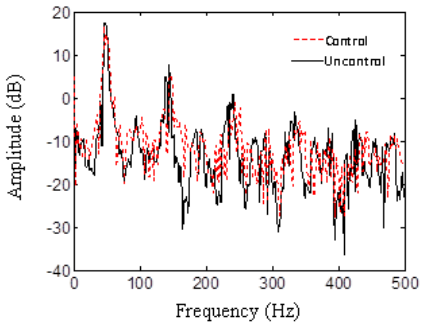

Figure 17 Experimental open-loop vs. closed-loop frequency response of Beam (a)

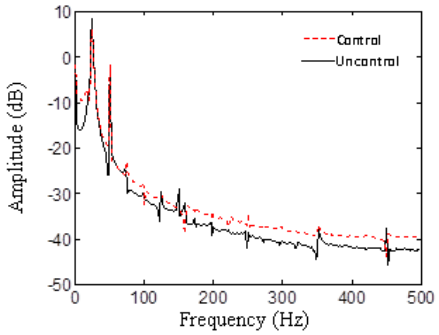

Figure 18 Experimental open-loop vs. closed-loop frequency response of Beam (b)

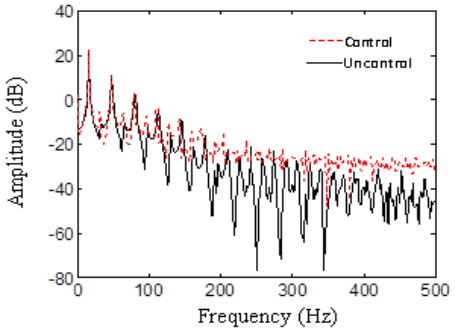

Figure 19 Experimental open-loop vs. closed-loop frequency response of Beam (c)

5 CONCLUSION

Vibration suppression of smart beams using the piezoelectric patch structure is presented in the paper. An experimental set-up has been developed to obtain the active vibration suppression of smart beam. Experiments are conducted to compare the controlling of various cantilever beams of different sizes. Experimentally the damping coefficient of the smart system has been determined and a state space model characterizing the dynamics of the physical system is developed from experimental results using PID approach for the purpose of control law design. Based on the PID controller, an experimental feedback controller has been designed and employed to determine the closed loop response of the system. It shows that the present actuator and sensor based control method is effective and the LabView control plots for various beams can be used as a benchmark for analytical work. The experimental results obtained by using the active vibration control system have demonstrated the validity and efficiency of PID controller. The experimental results are in good agreement with the results obtained using 2D-FE ABAQUS and 1D Finite element method based on zigzag theory.

References

[1] R.C. Averill and Y.C. Yip. Thick beam theory and finite element model with zigzag approximation. *AIAA J.*, 34:1626–32, 1996.

[2] A. Bagis. Determination of the pid controller parameters by modified genetic algorithm for improved performance. *Journal of Information Science and Engineering*, 23:1469–1480, 2007.

[3] A. Baz and S. Poh. Experimental implementation of the modified independent modal space control method. *Journal of sound and vibration*, 139(1):133–149, 1990.

[4] Qiu Cheng-Zhi, Han Da-Jian, Zhang Min-Xian, Wang Chao-Yue, and Wu Wei-Zhen. Active vibration control of a flexible beam using a non-collocated acceleration sensor and piezoelectric patch actuator. *Journal of Sound and Vibration*, 326:438–455, 2009.

[5] S.B. Choi and J.W. Sohn. Chattering alleviation in vibration control of smart beam structures using piezofilm actuators, experimental verification. *Journal of Sound and Vibration*, 294(3):640–649, 2006.

[6] S.S Ge, T. H. Lee, G. Zhu, and F. Hong. Variable structure control of a distributed parameter flexible beam. *Journal of Robotic systems*, 18(1):17–27, 2001.

[7] G.Gatti, M. J. Brennan, and P. Gardonio. Active damping of a beam using a physically collocated accelerometer and piezoelectric patch actuator. *Journal of Sound and Vibration*, 303(3-5):798–813, 2007.

[8] G.C. Goodwin, A.R. Woodyatt, R.H. Middleton, and J. Shim. Fundamental limitations due to jω- axis zeros in siso systems. *Automatica*, 35:857–63, 1999.

[9] S. Kapuria and N. Alam. Efficient layerwise finite element model for dynamic analysis of laminated piezoelectric beams. *Comput. Methods Appl. Mech. Engrg*, 195:2742–2760, 2006.

[10] S. Kapuria and Y. M. Yasin. Active vibration suppression of multilayered plates integrated with piezoelectric fiber reinforced composites using an efficient finite element model. *J. of Sound and Vibration*, 329(16):3247–3265, 2010.

[11] B.C. Kuo. *Automatic Control Systems*. Prentice Hall, 6th edition, 1991.

[12] W. Lianghong, W. Yaonan, Z. Shaowu, and T. Wen. Design of pid controller with incomplete derivation based on differential evolution algorithm. *Journal of Systems Engineering and Electronics*, 19(3):578–583, 2008.

[13] L. Meirovitch. *Dynamics and Control of Structure*. Wiley, New York, 1990.

[14] K. Ogata. *Modern Control Engineering*. Prentice Hall, 6th edition, 1997.

[15] M. Petyt. *Introduction to Finite Element Variation Analysis*. Cambridge University Press, Cambridge, 1990.

[16] A. Preumont. *Vibration Control of Active Structures*. Kluwer Academic Publishers, Dordrecht, 2004.

[17] D. Sun, J. Shan, and Y.X. Su. et al. Hybrid control of a rotational flexible beam using enhanced pd feedback with a nonlinear differentiator and pzt actuator. *Smart Materials & Structures*, 14(1):69–78, 2005.

[18] K. Szabat and T. Orlowska-Kowalska. Vibration suppression in a two-mass drive system using pi speed controller and additional feedbacks – comparative study. *IEEE Trans Ind Electron*, 54:1193–206, 2007.

[19] Li. Yang and Shi. Zhifei. Free vibration of a functionally graded piezoelectric beam via state-space based differential quadrature. *Composite Structures*, 87:257–264, 2009.

[20] A. Zabiullah, R. Sedagati, and R. Ganesan. Active vibration suppression of smart laminated beams using layerwise theory and an optimal control strategy. *Smart Materials and structures*, 16:2190–2201, 2007.